

Model complexes for ureases: a dinickel(II) complex with a novel asymmetric ligand and comparative kinetic studies on catalytically active zinc, cobalt, and nickel complexes

Birgit Hommerich, Hendrik Schwöppe, Dirk Volkmer, Bernt Krebs

Angaben zur Veröffentlichung / Publication details:

Hommerich, Birgit, Hendrik Schwöppe, Dirk Volkmer, and Bernt Krebs. 1999. "Model complexes for ureases: a dinickel(II) complex with a novel asymmetric ligand and comparative kinetic studies on catalytically active zinc, cobalt, and nickel complexes." *Zeitschrift für anorganische und allgemeine Chemie* 625 (1): 75–82.
[https://doi.org/10.1002/\(sici\)1521-3749\(199901\)625:1%3C75::aid-zaac75%3E3.0.co;2-x](https://doi.org/10.1002/(sici)1521-3749(199901)625:1%3C75::aid-zaac75%3E3.0.co;2-x).



Model Complexes for Ureases: A Dinickel(II) Complex with a Novel Asymmetric Ligand and Comparative Kinetic Studies on Catalytically Active Zinc, Cobalt, and Nickel Complexes

Birgit Hommerich, Hendrik Schwöppe, Dirk Volkmer*, and Bernt Krebs*

Münster, Anorganisch-Chemisches Institut der Universität

Dedicated to Professor Heinrich Nöth on the Occasion of his 70th Birthday

Abstract. The dinuclear nickel(II) complex of the asymmetric ligand 1-[*N,N*-bis(2-pyridylmethyl)amino]-3-[2-(3,5-dimethyl-1*H*-pyrazol-1-yl)ethoxy]-2-hydroxypropane (HL1) was prepared as a model for the active site of urease. The novel complex $[\text{Ni}_2(\text{L1})(\text{MeCOO})(\text{ClO}_4)(\text{EtOH})_2](\text{ClO}_4) \cdot 0.5 \text{Et}_2\text{O}$ (**1**) crystallizes in the triclinic space group *P* $\bar{1}$ with $a = 11.639(2)$ Å, $b = 12.571(3)$ Å, $c = 16.341(3)$ Å, $\alpha = 92.29^\circ$, $\beta = 106.54^\circ$, and $\gamma = 113.73^\circ$. The nickel ions (c.n. 6) are bridged by the alkoxy donor substituent of the ligand and an acetate anion. The dinuclear nickel(II), cobalt(II), and zinc(II) complexes of the ligands 1-[*N,N*-bis(2-benzimidazolylmethyl)amino]-3-[2-(3,5-dimethyl-1*H*-pyrazol-1-yl)ethoxy]-2-hydroxypropane (HL2), *N*-methyl-*N,N,N'*-tris(2-benzimidazolylmethyl)-2-hydroxy-1,3-diaminopropane (HL3), and

N,N,N',N'-tetrakis(2-benzimidazolylmethyl)-2-hydroxy-1,3-diaminopropane (HL4) were investigated for their activity towards the hydrolysis of the test substrate *p*-nitrophenyl acetate (npa) in ethanol-water (1:1). The second-order rate constants for the cleavage of npa were determined for all complexes. The profile of the pH dependence indicates that a hydroxide initially binds to the metal ion. The bound nucleophile subsequently attacks the test substrate. The results are discussed in terms of a refined model for the structure activity relationships of the dinuclear active site of urease.

Keywords: Urease; Nickel Complex; Hydrolysis; *p*-Nitrophenyl acetate

Modellkomplexe für Ureasen: Ein Dinickel(II)-Komplex mit einem neuen unsymmetrischen Liganden und vergleichende kinetische Untersuchungen mit katalytisch aktiven Zink-, Cobalt- und Nickelkomplexen

Inhaltsübersicht. Der dinukleare Nickel(II)-Komplex des asymmetrischen Liganden 1-[*N,N*-Bis(2-pyridylmethyl)amino]-3-[2-(3,5-dimethyl-1*H*-pyrazol-1-yl)ethoxy]-2-hydroxypropan (HL1) wurde als Modell für das aktive Zentrum der Urease synthetisiert. Der neue Komplex $[\text{Ni}_2(\text{L1})(\text{MeCOO})(\text{ClO}_4)(\text{EtOH})_2](\text{ClO}_4) \cdot 0.5 \text{Et}_2\text{O}$ (**1**) kristallisiert in der triklinen Raumgruppe *P* $\bar{1}$ mit $a = 11.639(2)$ Å, $b = 12.571(3)$ Å, $c = 16.341(3)$ Å, $\alpha = 92.29^\circ$, $\beta = 106.54^\circ$, und $\gamma = 113.73^\circ$. Die Nickelionen (K. Z. 6) sind durch den Alkoxy-Donorsubstituenten des Liganden und ein Acetation verbrückt. Die Aktivität der dinuklearen Nickel(II)-, Cobalt(II)- und

Zink(II)-Komplexe der Liganden 1-[*N,N*-Bis(2-benzimidazolylmethyl)amino]-3-[2-(3,5-dimethyl-1*H*-pyrazol-1-yl)ethoxy]-2-hydroxypropan (HL2), *N*-Methyl-*N,N,N'*-tris(2-benzimidazolylmethyl)-2-hydroxy-1,3-diaminopropan (HL3), und *N,N,N',N'*-Tetrakis(2-benzimidazolylmethyl)-2-hydroxy-1,3-diaminopropan (HL4) wurden in bezug auf die Hydrolyse von *p*-Nitrophenylacetat (npa) in Ethanol-Wasser (1:1) untersucht. Für die Spaltung von npa wurden für alle Komplexe die Geschwindigkeitskonstanten zweiter Ordnung bestimmt. Das pH-Abhängigkeitsprofil zeigt, daß ein Hydroxidion zunächst an das Metallion bindet. Das gebundene Nucleophil greift anschließend das Testsubstrat an. Die Ergebnisse werden im Hinblick auf ein verfeinertes Modell zur Struktur-Aktivitäts-Beziehung des zweikernigen aktiven Zentrums der Urease diskutiert.

* Prof. Dr. Bernt Krebs
Anorganisch-Chemisches Institut der Universität Münster
Wilhelm-Klemm-Str. 8
D-48149 Münster, Germany
Telefax: Int.cod + 25 18 33 83 66
e-mail: krebs@nwz.uni-muenster.de

* Dr. Dirk Volkmer
Anorganische Chemie I, Universität Bielefeld
Postfach 1001 31
D-33501 Bielefeld, Germany
e-mail: dvolkmer@uni-bielefeld.de

Introduction

The bond cleavage which proceeds through hydrolysis is among the most important reactions occurring in the biotic world. A large number of key metabolic com-

pounds (phosphate esters, amides, fatty acid esters) require an efficient catalysis of hydrolytic bond cleavage, which is almost always supported by metalloenzymes [1]. One of the most prominent cases is the hydrolysis of urea, the ubiquitous end product of dissimilative degradation of N-containing metabolites (amino acids, amino sugars, nucleobases) in mammals [2]. Spontaneous hydrolysis of urea is very slow, which points to an extraordinary stability: Compared to carboxylic acid esters the electron density of the urea carbonyl-C atom is significantly higher, thus increasing the activation barrier for nucleophilic attack [3]. Nature has addressed this problem by the unusual enzyme urease (EC 3.5.1.5), which is exceptional in several ways. First, it is so far the only known metalloenzyme which uses nickel(II) ions to perform a hydrolytic bond cleavage (a task usually covered by zinc-containing enzymes) [1, 4]. Second, it exhibits an extraordinary substrate specificity allowing catalytic turnover of only a few structurally very similar urea derivatives [5], and third, urease shows a very high catalytic proficiency [6].

Although a minimal mechanism for enzymatic urea cleavage was already proposed in 1980 by Zerner et al. [5], (see also reference [7]) equally efficient urea cleavage by nickel(II) ions or simple nickel(II) complexes has never been observed *in vitro*. The solution of the single crystal X-ray structure from native *Klebsiella aerogenes* urease and some of its derivatives has provided further insight into the possible mechanistic details [8]. Figure 1 schematically shows the structure of the dinuclear active site from *K. aerogenes* urease. Electron density mapping of the active site does not allow to determine the non-protein ligands of the nickel(II) ions beyond doubt. In the first paper in 1995, solely a single water ligand had been proposed to bind to Ni(2), resulting in two coordinatively highly unsaturated nickel(II) ions (3-/5-fold coordination environment) [9]. In a more recent paper the original suggestion has been reconsidered. According to present knowledge a further water (or hydroxide) ligand bridges the nickel ions and an additional water ligand coordinates to Ni(1) [8].

In view of our continuous efforts to model the structure and functional properties of urease, as well as those of other hydrolytically active metalloenzymes [10, 11], we here describe the synthesis and crystal structure of the new model compound $[\text{Ni}_2(\text{L}_1)(\text{MeCOO})(\text{ClO}_4)(\text{EtOH})_2](\text{ClO}_4) \cdot 0.5 \text{ Et}_2\text{O}$, (**1**), which bears a high structural similarity to the asymmetric dinuclear active site of urease. However, a structural feature that cannot be imitated easily by a simple model complex is the urea-specific hydrogen bonding pocket of the enzyme. It contributes significantly to decrease the energy for nucleophilic attack on the substrate (see Figure 1) [6, 9]. Not surprising, none of the model compounds examined so far shows

activity towards urea hydrolysis under biomimetic conditions, although one of the model compounds did show a pronounced stoichiometric activity towards phosphate ester hydrolysis [10b]. One compound was able to slowly cleave urea in ethanol at 80 °C [12b]. The missing activity of our compounds to promote

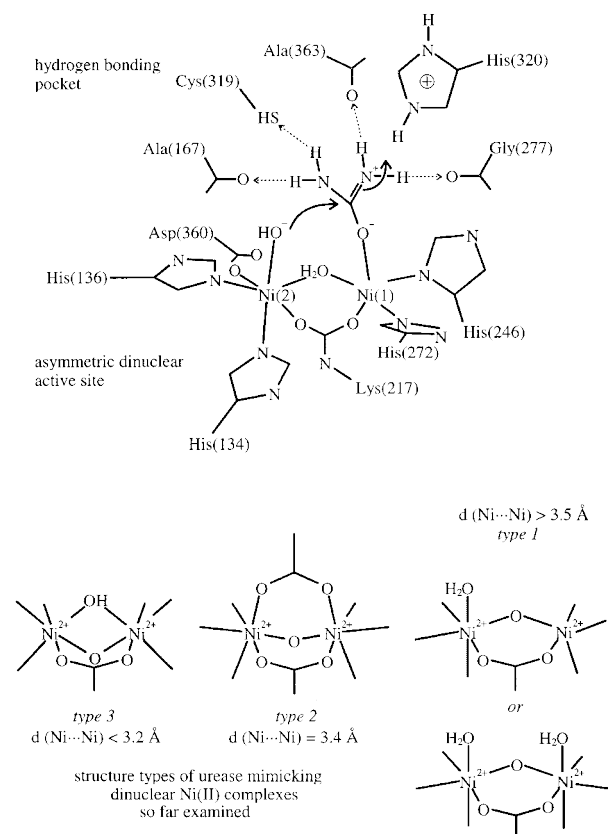


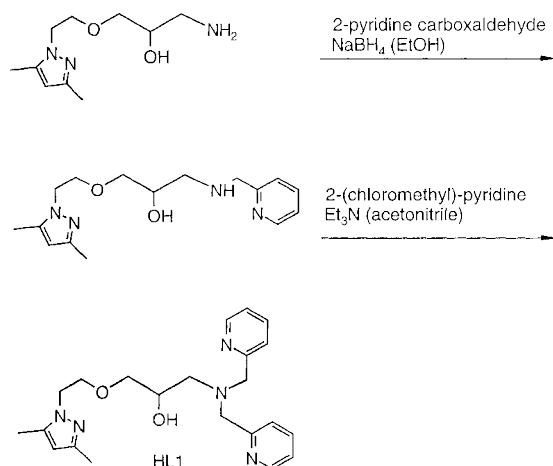
Fig. 1 Top: Excerpt of the dinuclear active site from *K. aerogenes* urease [6, 9] (PDB entry code: 1FWJ). Each Ni(II) is coordinated by two histidine residues (Ni(1): His(272), His(246); Ni(2): His(134), His(136). Ni(2) furthermore binds to an aspartate ligand (Asp(360)), thus rendering coordination of the metal ions in the dinuclear active site highly unsymmetrical. The Ni...Ni distance is 3.5 Å. A bridging carbamate stems from addition of CO_2 to a lysine residue (Lys(217)). The dinuclear active site mainly serves to efficiently transfer the nucleophilic attack of an OH^- on the urea carbonyl-C atom [5]. A fitted highly urea-specific hydrogen bonding pocket serves to prealign the coordinated urea substrate, thus lowering the energy for nucleophilic attack on it. Bottom: The present urease model is in very good agreement to the results of modelling studies on different types of carboxylate-bridged dinuclear nickel(II) complexes [10, 12]. The central μ_2 -alkoxo- μ_2 -carboxylato dinickel unit is well suited to constrain the positions of two opposing “free” ligand sites and thus to prevent unfavorable μ_2 -bridging of the hydroxide nucleophile (*type-3* structure). The non-substrate bound structure of urease as well as modelling studies would suggest that the most active catalyst could be expected for complexes with structures being constrained to an intermediate state of *type 1* or 2.

urea hydrolysis thus led us to search for a more sensitive test substrate. Here, we describe the hydrolysis of *p*-nitrophenyl acetate by a range of structurally different dinuclear nickel(II) complexes. The results are discussed in terms of structure-activity relationships for the proposed urease mechanism. Furthermore, catalytic studies were extended to the corresponding dinuclear zinc(II) and cobalt(II) derivatives of the ligands, hoping to shed some light on the preferential use of nickel(II) for urea hydrolysis.

Results and Discussion

Crystal Structure of **1**

The ligand HL1 was prepared according to the procedure represented in Scheme 1. After dropwise addition of a solution of HL1 to a solution of a 1:1 mixture of nickel(II) acetate and nickel(II) perchlorate, the compound $[\text{Ni}_2(\text{L1})(\text{MeCOO})(\text{ClO}_4)(\text{EtOH})_2] \cdot (\text{ClO}_4) \cdot 0.5 \text{Et}_2\text{O}$ (**1**) was obtained as a green crystalline solid.



Scheme 1 Reaction scheme for the synthesis of the asymmetric dinucleating ligand HL1

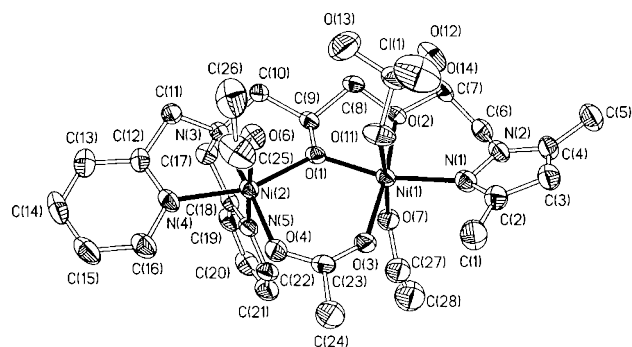


Fig. 2 Molecular structure and atomic numbering scheme for the cation of $[\text{Ni}_2(\text{L1})(\text{MeCOO})(\text{ClO}_4)(\text{EtOH})_2](\text{ClO}_4) \cdot 0.5 \text{C}_4\text{H}_{10}\text{O}$ **1**

The dinuclear complex **1** crystallizes in the triclinic space group $P\bar{1}$. The structure of the cation is shown in Figure 2, crystallographic details are given in Table 1, and selected bond lengths and angles are listed in Table 2.

The nickel(II) ions are bridged by the alkoxy donor atom of the ligand and a single acetate anion. Both nickel(II) atoms are in a distorted octahedral coordination environment comprising different kinds of do-

Table 1 Crystallographic details for $[\text{Ni}_2(\text{L1})(\text{MeCOO})(\text{ClO}_4)(\text{EtOH})_2](\text{ClO}_4) \cdot 0.5 \text{C}_4\text{H}_{10}\text{O}$ (**1**)

formula	$\text{C}_{32}\text{H}_{53}\text{N}_5\text{Cl}_2\text{Ni}_2\text{O}_{15}$
M_r , g · mol ⁻¹	936.12
space group	$P\bar{1}$ (no. 2)
a , Å	11.639(2)
b , Å	12.571(3)
c , Å	16.341(3)
α , deg	92.29(3)
β , deg	106.54(3)
γ , deg	113.73(3)
V , Å ³	2065.4(7)
Z	2
ρ_{calc} , g · cm ⁻³	1.505
crystal dimensions, mm	0.35 × 0.38 × 0.03
radiation	MoK α (0.71073 Å)
absorption coefficient, mm ⁻¹	1.108
T , °C	-123
scan type	ω scan
θ range, deg	2.02 – 27.12
index ranges	$0 \leq h \leq 14$; $-16 \leq k \leq 16$; $-20 \leq l \leq 20$
total data measured	9390
no. of reflns	8857
no. of variables	499
R [5458, $I > 2\sigma(I)$]:	$R_1^a = 0.0639$, $wR_2^b = 0.1718$
R (all data)	$R_1^a = 0.1041$, $wR_2^b = 0.1966$
GOF on F^2	0.948
min./max. diff. peaks, e ⁻ · Å ⁻³	1.49/−0.75

^a) $R_1 = \sum ||F_o| - |F_c|| / \sum |F_o|$; ^b) $wR_2 = [\sum w(F_o^2 - F_c^2)^2 / \sum wF_o^4]^{1/2}$; $w = 1/[\sigma^2(F_o^2) + (0.1209 P)^2]$; $P = (F_o^2 + 2F_c^2)/3$.

Table 2 Selected bond lengths (in Å) and angles (in deg) for **1**

Ni(1)···Ni(2)	3.531(2)	Ni(1)–O(1)	1.934(4)	Ni(2)–O(1)	1.990(3)
Ni(1)–O(2)	2.106(3)	Ni(2)–O(4)	2.007(4)		
Ni(1)–O(3)	2.025(3)	Ni(2)–O(6)	2.164(3)		
Ni(1)–O(7)	2.085(4)	Ni(2)–N(3)	2.102(4)		
Ni(1)–O(11)	2.303(4)	Ni(2)–N(4)	2.084(4)		
Ni(1)–N(1)	2.073(5)	Ni(2)–N(5)	2.065(4)		
Ni(1)–O(1)–Ni(2)	128.3(2)	O(1)–Ni(1)–O(2)	78.8(1)		
O(1)–Ni(2)–O(4)	99.6(2)				
O(1)–Ni(1)–O(3)	94.6(1)	O(1)–Ni(2)–O(6)	82.0(1)		
O(1)–Ni(1)–O(7)	95.0(2)	O(1)–Ni(2)–N(3)	83.5(2)		
O(1)–Ni(1)–O(11)	85.1(2)	O(1)–Ni(2)–N(4)	161.2(2)		
O(1)–Ni(1)–N(1)	164.5(2)	O(1)–Ni(2)–N(5)	93.0(2)		
O(2)–Ni(1)–O(3)	172.1(2)	O(4)–Ni(2)–O(6)	89.8(2)		
O(2)–Ni(1)–O(7)	86.5(1)	O(4)–Ni(2)–N(3)	176.4(2)		
O(2)–Ni(1)–O(11)	99.5(1)	O(4)–Ni(2)–N(4)	97.0(2)		
O(2)–Ni(1)–N(1)	90.8(2)	O(4)–Ni(2)–N(5)	95.8(2)		
O(3)–Ni(1)–O(7)	89.8(2)	O(6)–Ni(2)–N(3)	92.4(2)		
O(3)–Ni(1)–O(11)	83.9(1)	O(6)–Ni(2)–N(4)	89.4(2)		
O(3)–Ni(1)–N(1)	96.5(2)	O(6)–Ni(2)–N(5)	173.0(2)		
O(7)–Ni(1)–O(11)	173.8(1)	N(3)–Ni(2)–N(4)	80.1(2)		
O(7)–Ni(1)–N(1)	95.7(2)	N(3)–Ni(2)–N(5)	82.1(2)		
O(11)–Ni(1)–N(1)	85.4(2)	N(4)–Ni(2)–N(5)	93.9(2)		

nor atoms. Ni(1) is coordinated by a pyrazolyl nitrogen (N1), and two oxygen atoms (O(1), O(2)) of the ligand. Three additional oxygen atoms (O(3), O(7), O(11)) from the bridging acetate, the coordinated solvent ethanol and a monodentately bound perchlorate anion complete the coordination sphere. The coordination environment of Ni(2) consists of three nitrogen atoms (N(3), N(4), N(5)), one oxygen (O(1)) from the ligand and another two oxygen donor atoms (O(4)) and (O(6)), one from the bridging acetate and one from the second coordinated ethanol, respectively. Adding up the charges within the asymmetric unit of the cell indicates that the coordinated ethanol moieties are electrostatically neutral, i.e. protonated. This may also be verified by considering the Ni–O bond lengths: the X-ray structure analysis shows rather short Ni–O bond lengths in the range of 1.934–2.025 Å for the bridging anionic alkoxy and acetate donors (cf. Table 2). In comparison, the distances towards the coordinated neutral ethanol ligands Ni(1)–O(7) = 2.085 Å and Ni(2)–O(6) = 2.164 Å, are rather long.

The Ni(1)⋯Ni(2) distance of 3.531(2) Å fits well into the scheme considering a *type-I* structure of the central μ_2 -alkoxo- μ_2 -carboxylato dinickel unit, which is found to be almost planar (largest deviation from plane 0.057 Å for O(3)). Structures of similarly coordinated dinuclear complexes show one of the nickel(II) ions of the *type-I* structure to be five-coordinated [10b]. We notice here that an octahedral coordination for both nickel(II) ions, as in the structure of compound **1**, is possible, too. Hence, there seems to be no intrinsic preference for dinuclear μ_2 -oxo- μ_2 -carboxylato bridged nickel(II) complexes to adopt a low coordinated state for one of the metal ions. This could have been speculated from previously published model compounds, as well as from the proposed structure of the dinuclear active site from urease.

Electronic Absorption Properties

The nickel atoms of the dinuclear centre of **1** are coordinated differently (Ni(1): 5 O, 1 N; Ni(2): 3 O, 3 N donor environment). The electronic spectrum displays four absorption maxima at 597 ($\epsilon = 43.9$), 683 ($\epsilon = 42.3$), 775 ($\epsilon = 54.1$), and 978 nm ($\epsilon = 72.1 \text{ M}^{-1} \text{ cm}^{-1}$). Although the spectrum shows similarities to those of octahedrally coordinated nickel(II) ions, it is not unequivocally possible to assign the bands to the spin-allowed transitions from the $^2A_{2g}$ ground state of an octahedral d^8 ion to the next higher excited triplet states ($^3T_{1g}$ (P), $^3T_{1g}$ (F), and $^3T_{2g}$ (F)). The complex shows a large shift of the band maxima and relatively high molar extinction coefficients if compared to the nickel(II) hexaaqua cation. This may be due to the fact that the coordination environment of each of the

nickel(II) ions clearly deviates from strictly octahedral symmetry [13].

As yet we have not found any suitable model to deduce the average donor environment of the nickel(II) ions simply by examining the UV-vis band maxima and intensities of the spectra. This severely limits the value of this method for structure prediction in the case of urease. The problem arose at a point when we were trying to develop a spectroscopic method to determine the number of “free” ligand sites in our complexes [14].

We were hoping to find a suitable spectroscopic probe which would exclusively and quantitatively replace the coordinated water or alcohol ligands in the present complexes, at the same time leading to a spectral shift from which we could follow the course of the ligand exchange. While in the case of copper(II) complexes azide titrations are commonly used for that purpose [15], we could not succeed with this method in the case of the present nickel(II) complexes. The spectral shift of the *d–d* transitions was simply too small to allow quantitative evaluation.

To get at least an idea if the dinuclear complexes are stable under the conditions of the kinetic investigations, further spectrophotometric titrations were carried out. We observed the π - π^* -bands of the ligands in the range of 230–290 nm during the addition of metal salt to the solution. As an example, Figure 3 shows the titration of HL2 with $[\text{Ni}(\text{H}_2\text{O})_6](\text{NO}_3)_2$ in ethanol-water (1 : 1) (pH 6.73, 20 °C). The spectrum of HL2 (dashed lines) displays four maxima ($\lambda_{\text{max}}^1 = 281.9 \text{ nm}$, $\lambda_{\text{max}}^2 = 275 \text{ nm}$, $\lambda_{\text{max}}^3 = 249.6 \text{ nm}$, $\lambda_{\text{max}}^4 = 245.4 \text{ nm}$). After the addition of $[\text{Ni}(\text{H}_2\text{O})_6](\text{NO}_3)_2$ a band shift of 2 nm towards shorter wavelengths of the λ^1 - and λ^2 -bands was observed. In addition, a change in extinction of all maxima occurred. The spectrophotometric titration was complete after having added two equivalents of nickel(II) ions. No additional changes in intensities or band shifts occurred when the nickel(II) concentration was further increased. The titration spectrum showed three isosbestic points ($\lambda_{\text{iso}}^1 = 277.9 \text{ nm}$, $\lambda_{\text{iso}}^2 = 266.0 \text{ nm}$, $\lambda_{\text{iso}}^3 = 262.5 \text{ nm}$).

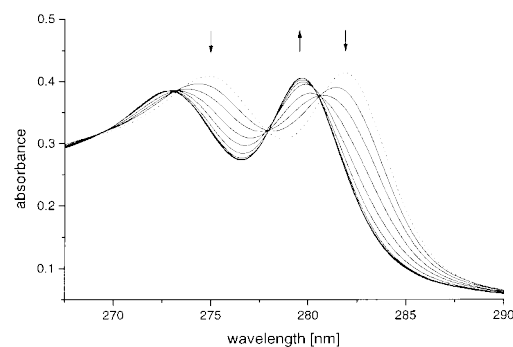


Fig. 3 Spectrophotometric titration of HL2 with $[\text{Ni}(\text{H}_2\text{O})_6](\text{NO}_3)_2$ in ethanol-water (1 : 1) at pH 6.73

The *in situ* formed nickel(II) complexes of HL3 and HL4 as well as the cobalt(II) and zinc(II) complexes of the investigated ligands showed similar behavior. The results are in agreement with the assumption that dinuclear complexes of HL2–HL4 preferentially form at a $[\text{Ni}(\text{H}_2\text{O})_6]^{2+}/\text{HL2}$ ratio of 2:1 under the conditions of the kinetic investigations as described in the following section. However, these results naturally do not provide structural evidence for the precise coordination properties of the metal ions in the dinuclear complexes.

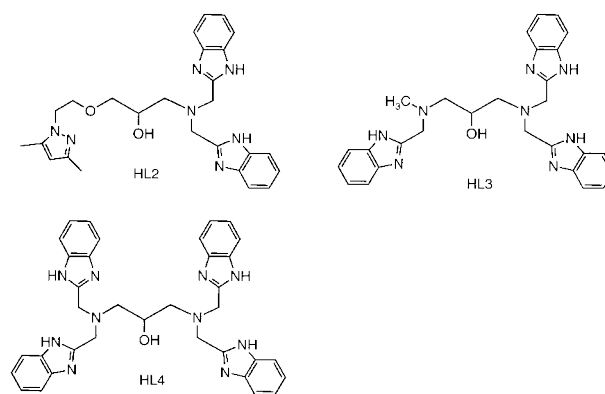
Kinetic Investigations

One of the most remarkable features of urease is the use of nickel(II) ions to perform hydrolysis. The most appropriate way to find an explanation for this would be to examine hetero metal derivatives of the apoenzyme, to study the modified reaction rates and the altered pH profile of the catalytic behavior. However, the preparation as well as the characterization of metal-exchanged urease does not seem to be straightforward [16]. Here, biomimetic model complexes may offer a suitable alternative to study systematic variations. As a first step into this direction we decided to investigate the behavior of selected metal complexes towards their hydrolytic activity of a suitable test substrate. The ligands we chose differed by the kind and number of donor groups on one metal coordination site. The other site always consisted of the bis(2-benzimidazolymethyl)amino group (cf. Scheme 2).

To initiate studies, we refrained from using complexes that were completely characterized by X-ray crystallography. The expenditure for synthesizing all metal derivatives of the chosen ligands would not have been justified, since the solid state structure of the coordinatively labile complexes would not prove their existence in solution. Therefore, the dinuclear cobalt(II), nickel(II), and zinc(II) complexes of the ligands HL2–HL4 (Scheme 2) were prepared *in situ*, just by adding metal salts and ligand in a 2:1 ratio to the buffered solution. Due to solubility problems metal complexes of the ligand HL1 could not be taken into account for the kinetic investigations. Initial rate experiments were performed to test the ability of the complexes to hydrolyze *p*-nitrophenyl acetate (npa). Npa has been used as a test substrate for ureolytic activity before, keeping in mind the fact that it is *not* a natural substrate for the enzyme urease [17]. The complete literature on the use of npa as a test substrate for hydrolytic activity cannot be reviewed here [18]. The choice of npa simply arose from the fact, that the more appropriate test substrates such as *p*-nitrophenyl urea or *N,N'*-di(*p*-nitrophenyl) urea were just too stable against hydrolytic cleavage which shifted the necessary observation times into unacceptable limits. In order to examine the delicate influence

of different metal ions, ligands, pH, electrolyte concentrations and temperature, the choice of the hydrolytically much less stable npa seems to be justified. Besides, npa as a model substrate imitates well the planar sp^2 -hybridized system of urea. Its hydrolysis product (*p*-nitrophenolate (npat)) is easily detectable by following the change in absorption at 400 nm ($\epsilon_{400}^0 = 18700 \text{ M}^{-1} \text{ cm}^{-1}$).

As an example, the initial rates of hydrolysis of npa by $[\text{Zn}_2(\text{L2})]^{n+}$ ($t < 5 \text{ min}$, 5 mM $[\text{Zn}_2(\text{L2})]^{n+}$, pH 6.54, 20 °C) at various substrate concentrations are displayed in Figure 4. In the range of 5–50 mM of npa, a



Scheme 2 Ligands used for the kinetic investigations

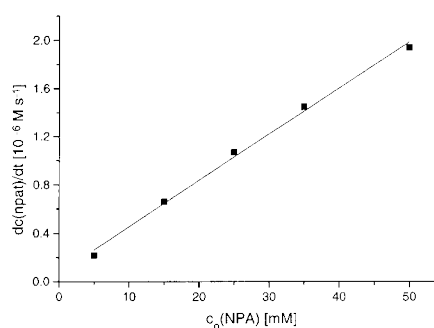


Fig. 4 Hydrolysis of *p*-nitrophenyl acetate (npa) by $[\text{Zn}_2(\text{L2})]$ (5 mM) in ethanol-water (1:1) at pH 6.54 [buffer: 100 mM 3-[*N*-morpholino]propane sulfonic acid (MOPS)] and 20 °C, ($t < 5 \text{ min}$)

Table 3 Second-order rate constants (k_2) for the hydrolysis of *p*-nitrophenyl acetate by different metal complexes in ethanol-water (1:1), pH 6.52, 20 °C

M ²⁺	ligand	k ₂ (10 ⁻³ M ⁻¹ s ⁻¹)	M ²⁺	ligand	k ₂ (10 ⁻³ M ⁻¹ s ⁻¹)
Co	HL2	3.7	Zn	HL2	7.0
	HL3	8.4		HL3	23.9
	HL4	13.8		HL4	17.4
Ni	HL2	1.9	Co	(-)	0.8
	HL3	2.1	Ni	(-)	1.46
	HL4	3.6	Zn	(-)	0.9
			(-)	(-)	0.8

linear increase was observed. The nickel(II) and cobalt(II) complexes of the ligand HL2 as well as the complexes of HL3 and HL4 for all investigated metal ions show comparable behavior.

A linear dependence was also observed upon varying the concentration of the complex within the range of 1.5–5 mM, while precipitation occurred at higher concentrations. These results strongly indicate second-order kinetic behavior of the system under the chosen conditions. A similar behavior has also been found for structurally different dinuclear complexes earlier [19]. The second-order rate constants, k_2 , for the hydrolysis of npa by the nickel(II), cobalt(II), and zinc(II) complexes at pH 6.52 and 20 °C are shown in Table 3. (The copper(II) complexes of the ligands HL2–HL4 could not be examined due to the formation of precipitates under the conditions of the kinetic investigations.)

The activity of the complexes for a chosen ligand decreases in the order $\text{Zn}^{2+} > \text{Co}^{2+} > \text{Ni}^{2+}$ in all cases. This systematic behavior may be ascribed to two principles, which both take effect into the same direction. First, the kinetic exchange for coordinated water molecules is fastest for hydrated zinc(II) ions and slowest for nickel(II) ions [20]. If it is assumed that the exchange of water against the substrate npa follows the same trend, obviously hydrolysis should proceed faster for zinc than for nickel as the promoting metal ion. Second, the reaction rate is limited by the concentration of the nucleophile, e.g. coordinated hydroxide anions. At a given pH the acidity of the coordinated water molecule depends on the total charge of the metal cation, the coordination geometry and environment and its electronegativity [21]. If we only consider metal cations having the same formal charge (here +2 for all cations), and we would furthermore assume that the coordination geometries of the different cations for a selected ligand are equal, then the acidity of the coordinated water molecule would mainly depend on the electronegativity of the metals. Simply speaking: the hardest and less electronegative metal cation shows the greatest tendency to acidify the coordinated water molecule. Since in the Allred-Rochow scale the succession of electronegativities is $\text{Zn} (\chi^0 = 1.66) < \text{Co} (\chi^0 = 1.75) < \text{Ni} (\chi^0 = 1.80)$, a water molecule which is coordinated to a zinc(II) cation would deprotonate at comparably lower pH than within the corresponding nickel(II) complex [22].

The results of the kinetic measurements are in good agreement with these general considerations. If we compare the rate constants of the metal cations depending on the ligand structures, the activity of the cobalt(II) and nickel(II) complexes increases for all ligands with the number of benzimidazolyl groups. The zinc(II) complexes display a different result. In this case the complex of HL3 shows a higher activity than the zinc complex of HL4.

However, with respect to the missing structural parameters for the compounds further interpretations do not seem reasonable.

Instead, we took a closer look on the pH-dependencies of the catalysts. Figure 5 shows the pH dependence illustrated by the representative example $[\text{Ni}_2(\text{L2})]^{n+}$. The activity is low in the pH range < 7.2 and increases at higher pH. Similar results are found for the Co^{2+} and Zn^{2+} series but shifted to lower pH values.

We assume that the increasing hydrolytic activity of the complexes at higher pH values goes hand in hand with an increasing concentration of a coordinated hydroxide species in solution, which attacks the substrate as a nucleophile. The results so far obtained are in agreement with a cooperative hydrolysis mechanism, which requires a dinuclear catalyst. Although the achieved rate accelerations for npa hydrolysis are rather low (the maximum being 30 fold for $[\text{Zn}_2(\text{L3})]^{n+}$ at pH 6.52 as compared to spontaneous hydrolysis), the method seems to be appropriate to study the hydrolysis reactions by dinuclear model complexes.

Facing these results, one possible answer for the preferential use of nickel(II) instead of zinc(II) in urease could be that nickel ions match better the pH profile of the apoenzyme. The pH optimum for urease is at 7.75 [23]. At such a pH water molecules which are coordinated to zinc(II) are almost completely converted to hydroxide. This would be favorable in the sense of creating a high concentration of the nucleophile, but it would also cause the problem that urea would have to compete with a strongly bound hydroxide instead of a labile water at the second “free” coordination site. However, experimental evidence yet is too preliminary to underline this hypothesis. Future studies will address this general point of hydrolysis catalysis considering structurally more suitable biomimetic metal complexes, providing asymmetric dinuclear sites.

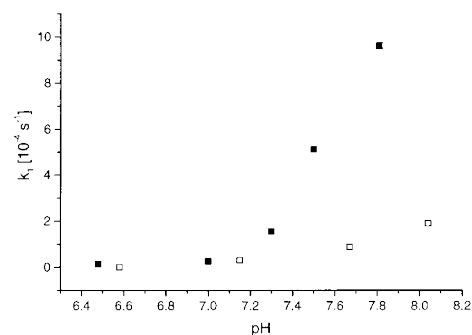


Fig. 5 Hydrolysis of *p*-nitrophenyl acetate (npa, 25 mM) by $[\text{Ni}_2(\text{L2})]$ (5 mM) (black) and nickel nitrate (10 mM) (open squares) in ethanol-water (1:1) [buffer: 100 mM 3-[N-morpholino]-propane sulfonic acid (MOPS) for pH < 7.5 ; 100 mM tris-(cyclohexylamino)methane (TRIS) for pH > 7.5] at 20 °C, ($t < 5$ min)

Experimental Section

General: Starting materials were purchased from commercial sources and were used without further purification. Solvents were dried using standard laboratory techniques. Melting points were determined by using a Mettler melting point apparatus (FP51). Elemental analyses were performed on a Hewlett Packard Scientific Model 185 instrument. ^1H and ^{13}C NMR spectra were recorded on Bruker WH300 and WH90 spectrometers. ^1H chemical shifts of the compounds are related to TMS as an internal standard for the deuterated solvent.

Preparation: 1-Amino-3-[2-(3,5-dimethyl-1H-pyrazol-1-yl)ethoxy]-2-hydroxypropane, 1-[N,N-bis(2-benzimidazolylmethyl)amino]-3-[2-(3,5-dimethyl-1H-pyrazol-1-yl)ethoxy]-2-hydroxypropane (HL2), N-methyl-N,N',N'-tris(2-benzimidazolylmethyl)-2-hydroxy-1,3-diaminopropane (HL3), and N,N,N',N'-tetrakis(2-benzimidazolylmethyl)-2-hydroxy-1,3-diaminopropane (HL4) were prepared as previously described [10]. The asymmetric ligand HL1 was prepared according to the procedure represented in Scheme 1.

1-[N-(2-Pyridylmethyl)amino]-3-[2-(3,5-dimethyl-1H-pyrazol-1-yl)ethoxy]-2-hydroxypropane: A sample of 1-amino-3-[2-(3,5-dimethyl-1H-pyrazol-1-yl)ethoxy]-2-hydroxypropane (10 g, 47 mmol) was dissolved in 30 mL of ethanol. Pyridine-2-carbaldehyde (5.885 g, 55 mmol) was added at room temperature. The yellow solution was heated to 50 °C and stirred for another 30 min. The resulting Schiff base was reduced with NaBH_4 and the reaction product was purified according to the published procedure [10]. Yield: 14.08 g (46.3 mmol, 98.5%); M. p. 51 °C.

^1H NMR (300 MHz, CDCl_3 , 25 °C): δ = 8.54 (m, 1 H, $-\text{C}_{\text{ar}}\text{H}$), 7.63 (m, 1 H, $-\text{C}_{\text{ar}}\text{H}$), 7.28 (m, 1 H, $-\text{C}_{\text{ar}}\text{H}$), 7.15 (m, 1 H, $-\text{C}_{\text{ar}}\text{H}$), 5.75 (s, 1 H, $-\text{C}_{\text{ar}}\text{H}$), 4.11 (m, 2 H, $-\text{CH}_2$), 3.90 (s, 2 H, $-\text{CH}_2$), 3.81 (m, 3 H, $-\text{CH}_2$, $-\text{CH}$), 3.44 (m, 2 H, $-\text{CH}_2$), 2.66 (m, 2 H, $-\text{CH}_2$), 2.21 (s, 3 H, $-\text{CH}_3$), 2.19 (s, 3 H, $-\text{CH}_3$); MS (70 eV, EI): m/z (%): 304 (16.3) [M^+].

$\text{C}_{16}\text{H}_{24}\text{N}_4\text{O}_2$ (304.4): calcd C 63.12, H 7.96, N 18.41; found C 63.56, H 7.74, N 18.78%.

1-[N,N-Bis(2-pyridylmethyl)amino]-3-[2-(3,5-dimethyl-1H-pyrazol-1-yl)ethoxy]-2-hydroxypropane (HL1): A sample of 2-(chloromethyl)pyridine hydrochloride (2.61 g, 15.9 mmol) was suspended in 12.5 mL of dry acetonitrile. After the suspension had been cooled to 0 °C, a cold solution of triethylamine (2.22 mL, 15.9 mmol) was added. The filtrate of the suspension was directly added to a solution of 1-[N-(2-pyridylmethyl)amino]-3-[2-(3,5-dimethyl-1H-pyrazol-1-yl)ethoxy]-2-hydroxypropane (4.38 g, 14.4 mmol) and triethylamine (1.12 mL, 15.2 mmol) in 50 mL of acetonitrile and the solution was refluxed for 3 h. The volume of the solution was reduced and the precipitated triethylamine hydrochloride was filtered off. The filtrate was stirred with a cooled saturated solution of potassium carbonate and extracted three times with CHCl_3 . The organic extract was dried over magnesium sulfate. The solvent was removed with a rotary evaporator and purified by column chromatography with silica gel (eluent: THF/MeOH (3:1)). Yellow oil, yield 0.85 g (2.15 mmol, 14.9%).

^1H NMR (300 MHz, CDCl_3 , 25 °C): δ = 8.53 (m, 2 H, $-\text{C}_{\text{ar}}\text{H}$), 7.58 (m, 2 H, $-\text{C}_{\text{ar}}\text{H}$), 7.29 (m, 2 H, $-\text{C}_{\text{ar}}\text{H}$), 7.13 (m, 2 H, $-\text{C}_{\text{ar}}\text{H}$), 5.71 (s, 1 H, $-\text{C}_{\text{ar}}\text{H}$), 3.97 (t, 2 H, $-\text{CH}_2$), 3.90 (q, 4 H, $2 \times -\text{CH}_2$), 3.76 (m, 3 H, $-\text{CH}_2$, $-\text{CH}$), 3.38 (d, 2 H, $-\text{CH}_2$), 2.71 (m, 2 H, $-\text{CH}_2$), 2.17 (s, 6 H, $2 \times -\text{CH}_3$); MS (70 eV, EI): m/z (%): 395 (22.7) [M^+].

$\text{C}_{22}\text{H}_{29}\text{N}_5\text{O}_2$ (395.6): calcd C 66.80, H 7.40, N 17.71; found C 66.55, H 7.64, N 17.87%.

$[\text{Ni}_2(\text{L1})(\text{MeCOO})(\text{ClO}_4)(\text{EtOH})_2](\text{ClO}_4) \cdot 0.5 \text{Et}_2\text{O}$ (1): A hot ethanolic solution of HL1 (116 mg, 0.29 mmol) was added dropwise to a hot solution of $[\text{Ni}(\text{H}_2\text{O})_6](\text{ClO}_4)_2$ (107 mg, 0.29 mmol) and $[\text{Ni}(\text{MeCOO})_2(\text{H}_2\text{O})_4]$ (71 mg, 0.29 mmol) in 5 mL of ethanol. The clear solution was refluxed for 5 min. The cooled solution was filtered. Slow vapor diffusion of diethyl ether into the filtrate at 4 °C gave green crystals of **1** which are sensitive towards loss of solvent. $\text{C}_{29.75}\text{H}_{48}\text{N}_5\text{Cl}_2\text{Ni}_2\text{O}_{14.5}$ (896.1): calcd C 37.63, H 4.66, N 8.52 (without ether); found C 34.68, H 4.95, N 7.89%.

X-ray Crystallography. Crystal data as well as details of data collection and refinement are summarized in Table 1 [24]. A single crystal of **1** was covered with a protective coating of mineral oil, mounted on a glass fiber, and placed on a SynTex P2₁ diffractometer (MoK α , λ = 0.71073 Å, graphite monochromator). The crystal was immediately cooled by a stream of dry nitrogen gas to avoid decomposition through the loss of solvent molecules. Cell constants and orientation matrices were determined using least-squares refinements of the angular coordinates of 20 accurately centered reflections. Intensity data were collected by using the ω -scan technique to a maximum 2θ value of 54°. As a check of crystal stability, two representative reflections were measured every 100 data points.

The structure was solved using direct methods (SHELXTL PLUS program package). Atomic scattering factors were taken from the *International Tables* [25]. The positions and anisotropic thermal parameters of all non-H atoms were refined against F_o^2 using full-matrix least squares techniques (SHELXL-93 program [26]). Hydrogen atoms were included in calculated positions with their bonding distances and thermal parameters depending on the pivot atom (H-C(sp²) 0.95 Å, $U_{\text{H}} = 1.2 U_{\text{eq}}$ (C); H-C(sp³, CH₂ group) 0.99 Å, $U_{\text{H}} = 1.2 U_{\text{eq}}$ (C); H-C(sp³, CH₃ group) 0.98 Å, $U_{\text{H}} = 1.5 U_{\text{eq}}$ (C); H-N(sp²) 0.88 Å, $U_{\text{H}} = 1.2 U_{\text{eq}}$ (N)). Positions of H atoms from disordered structure fragments were not included.

UV-Vis Spectroscopic Measurements and Kinetic Investigations. The electronic absorption spectrum of complex **1** was recorded on a Shimadzu UV 3100 PC spectrophotometer using a 0.01 M ethanolic solution (1 cm optical pathway). The spectrophotometric titration (Fig. 2) was observed by following the π - π^* -bands of the ligand in the range of 230–290 nm. A solution of $3 \cdot 10^{-5}$ M HL2 in ethanol-water (1:1) without buffer was titrated with 0.2 equivalents of $[\text{Ni}(\text{H}_2\text{O})_6](\text{NO}_3)_2$. The error caused by increase in volume was corrected.

The hydrolysis rate of npa was measured by following the increase of the absorption at 400 nm of the released 4-nitrophenolate. The reactions were carried out in ethanol-water mixtures (1:1) at 25 °C. The biological buffers MOPS and TRIS were used to maintain a constant pH in the range 6.5–8.5. The pHs of the solutions were adjusted with NaOH or HNO₃ and corrected according to literature recommendations for ethanol-water (1:1) mixtures [27]. The initial rate was determined by recording the absorbance at 400 nm for a period <5 minutes immediately after having added the substrate. The pH value was controlled after monitoring the release of *p*-nitrophenolate. Since at an approximate pH 7 yel-

low *p*-nitrophenolate and colorless *p*-nitrophenol are in pH-dependent equilibrium, the total concentration in these reaction solutions was calculated using ϵ_{400} (*p*-nitrophenolate) = 18700 M⁻¹ cm⁻¹ and pK_a (*p*-nitrophenol, 25 °C) = 7.15 [28]. The release of *p*-nitrophenolate with time showed a linear increase in all cases. All data in Table 3 were corrected for spontaneous hydrolysis of npa in the absence of any complex. A linear dependence of reaction rate (dc/dt) on npa concentrations was found (Fig. 4). The obtained second-order rate constants k_2 were calculated from $k_2 = (dc/dt) [npa]_{t=0}^{-1} [\text{complex}]^{-1}$ (Table 3).

The pH dependence (Fig. 5) of the hydrolysis of npa (25 mM) by [Ni₂(L2)]ⁿ⁺ (5 mM) at 20 °C was investigated as described above. The buffers MOPS and TRIS (100 mM) were used for pH < 7.5 and > 7.5, respectively. The combination of TRIS and metal ions alone shows some catalytic activity, but the investigated complexes are much faster. The k_1 values were calculated from $k_{\text{obs}} = \ln([npa]_{t=0}/([npa]_{t=0} - [npa]_t)) \cdot t^{-1} = k_1 + k_{\text{spont}}$; $k_1 = k_{\text{obs}} - k_{\text{spont}}$ (k_{spont} = rate constant for spontaneous hydrolysis of 4-nitrophenolate).

All kinetic experiments were run at least twice, with a reproducibility of 20%.

Acknowledgments: We thank Dr. Friedhelm Rogel for his assistance and for fruitful discussions. This work was supported by the Deutsche Forschungsgemeinschaft and the Fonds der Chemischen Industrie.

References

- [1] a) N. Sträter, W. N. Lipscomb, T. Klabunde, B. Krebs, *Angew. Chem.* **1996**, 108, 2158; *Angew. Chem. Int. Ed. Engl.* **1996**, 35, 2024; b) W. N. Lipscomb, N. Sträter, *Chem. Rev.* **1996**, 96, 2375.
- [2] M. Takiguchi, M. Mori, *Biochem. J.* **1995**, 312, 649.
- [3] B. Zerner, *Bioorg. Chem.* **1991**, 19, 116.
- [4] a) A. Taylor, *Trends Biochem. Sci.* **1993**, 18, 167; *FASEB J.* **1993**, 7, 290; b) B. L. Vallee, D. S. Auld, *Acc. Chem. Res.* **1993**, 26, 543.
- [5] N. E. Dixon, P. W. Riddles, C. Gazzola, R. L. Blakeley, B. Zerner, *Can. J. Biochem.* **1980**, 58, 1335; *ebenda* **1981**, 59, 564 (erratum).
- [6] P. A. Karplus, M. A. Pearson, R. P. Hausinger, *Acc. Chem. Res.* **1997**, 30, 330.
- [7] M. J. Todd, R. P. Hausinger, *J. Biol. Chem.* **1989**, 264, 15835.
- [8] M. A. Pearson, L. O. Michel, R. P. Hausinger, P. A. Karplus, *Biochemistry* **1997**, 36, 8164.
- [9] E. Jabri, M. B. Carr, R. P. Hausinger, P. A. Karplus, *Science* **1995**, 268, 998.
- [10] a) D. Volkmer, A. Hörstmann, K. Griesar, W. Haase, B. Krebs, *Inorg. Chem.* **1996**, 35, 1132; b) D. Volkmer, B. Hommerich, K. Griesar, W. Haase, B. Krebs, *Inorg. Chem.* **1996**, 35, 3792.
- [11] a) S. Uhlenbrock, R. Wegner, B. Krebs, *J. Chem. Soc., Dalton Trans.* **1996**, 3731; b) B. Krebs in: *Bioinorganic Chemistry – An Inorganic Perspective of Life*, D. P. Kessissoglou (Ed.), Kluwer Acad. Publ., Dordrecht–Boston–London 1995, pp. 371–384; c) S. Uhlenbrock, B. Krebs, *Angew. Chem.* **1992**, 104, 1631; *Angew. Chem. Int. Ed. Engl.* **1992**, 31, 1697; d) B. Bremer, K. Schepers, P. Fleischhauer, W. Haase, G. Henkel, B. Krebs, *J. Chem. Soc., Chem. Commun.* **1991**, 510.
- [12] a) R. M. Buchanan, M. S. Mashuta, K. J. Oberhausen, J. F. Richardson, Q. Li, D. N. Hendrickson, *J. Am. Chem. Soc.* **1989**, 111, 4497; b) K. Yamaguchi, S. Koshino, F. Akagi, M. Suzuki, A. Uehara, S. Suzuki, *J. Am. Chem. Soc.* **1997**, 119, 5752; c) T. Koga, H. Furutachi, T. Nakamura, N. Fukita, M. Ohba, K. Takahashi, H. Okawa, *Inorg. Chem.* **1998**, 37, 989; d) F. Meyer, A. Jacobi, B. Nuber, P. Rutsch, L. Zsolnai, *Inorg. Chem.* **1998**, 37, 1213.
- [13] A. E. Underhill, D. E. Billing, *Nature* **1966**, 210, 834.
- [14] D. Volkmer, B. Krebs, A. G. Sykes, *unpublished results*.
- [15] a) M. R. Oberholzer, M. Neuburger, M. Zehnder, T. A. Kaden, *Helv. Chim. Acta* **1995**, 78, 505; b) L. Casella, O. Carugo, M. Gullotti, S. Garofani, P. Zanello, *Inorg. Chem.* **1993**, 32, 2056.
- [16] G. J. King, B. Zerner, *Inorg. Chim. Acta* **1997**, 255, 381.
- [17] C. A. Salata, M.-T. Youinou, C. J. Burrows, *Inorg. Chem.* **1991**, 30, 3454.
- [18] a) E. Kimura, I. Nakamura, T. Koike, M. Shionoya, Y. Kodama, T. Ikeda, M. Shiro, *J. Am. Chem. Soc.* **1994**, 116, 4764; b) M. Ruf, K. Weis, H. Vahrenkamp, *J. Chem. Soc., Chem. Commun.* **1994**, 135.
- [19] a) J. Chin, X. Zou, *J. Am. Chem. Soc.* **1984**, 106, 3687; b) E. Kimura, T. Shiota, T. Koike, M. Shiro, M. Kodama, *J. Am. Chem. Soc.* **1990**, 112, 5805; c) C. Wendelstorf, S. Warzeska, E. Kövari, R. Krämer, *J. Chem. Soc., Dalton Trans.* **1996**, 3087.
- [20] H. Krüger, *Chem. Soc. Rev.* **1982**, 11, 227.
- [21] J. Livage, M. Henry, C. Sanchez, *Prog. Solid. St. Chem.* **1988**, 18, 259.
- [22] M. Henry, J. P. Jolivet, J. Livage, *Structure and Bonding* **1992**, 77, 153.
- [23] M. J. Todd, R. P. Hausinger, *J. Biol. Chem.* **1987**, 262, 5963.
- [24] Crystallographic data for the structure reported in this paper have been deposited with the Cambridge Data Centre as supplementary publication no. CCDC-100921. Copies of the data can be obtained free of charge on application to CCDC, 12 Union Road, Cambridge CB2 1EZ, UK [Fax: int. Code +44(1223)336-033; E-mail: deposit@ccdc.cam.ac.uk].
- [25] *International Tables for X-Ray Crystallography*, Vol. 4, Kynoch Press, Birmingham, U.K., **1974**.
- [26] G. M. Sheldrick, SHELXL-93, *Program for the Refinement of Crystal Structures*, Universität Göttingen, **1993**.
- [27] R. G. Bates, *Determination of pH*, 2nd edn., Wiley, New York, **1964**, p. 41; (pH = pH meter reading – 0.2).
- [28] M. M. Fickling, A. Fischer, B. R. Mann, J. Packer, J. Vaughan, *J. Am. Chem. Soc.* **1959**, 81, 4226.